Dimerization kinetics of the IgE-class antibodies by divalent haptens

I. The Fab-hapten interactions

Reinhard Schweitzer-Stenner,* Arieh Licht,‡ and Israel Pecht‡

*Institute of Experimental Physics, University of Bremen, 2800 Bremen 33, Germany; and ‡Department of Chemical Immunology, The Weizmann Institute of Science, Rehovot 76100, Israel

ABSTRACT The binding of divalent haptens to IgE-class antibodies leads predominantly to their oligomerization into open and closed dimers. Kinetics of the open dimer formation was investigated by fluorescence titrations of Fab fragments of monoclonal DNP-specific IgE antibodies with divalent haptens having different spacer length (Γ = 14–130 Å). Binding was monitored by quenching of intrinsic trytophan emission of the Fab. Addition of divalent haptens with short spacers (Γ = 14–21 Å) to the Fabs at rates larger than a distinct threshold value caused a significant decrease of Fab-binding site occupation in the initial phase of the titration. This finding was interpreted to reflect a nonequilibrium state of hapten-Fab-binding. Such nonequilibrium titrations were analyzed by inserting a kinetic model into a theory of antibody aggregation as presented by Dembo and Golstein (Histamine release due to bivalent penicilloyl haptens. 1978. *J. Immunol.* 121, 345). Fitting of this model to the fluorescence titrations yielded dissociation rate constants of $7.8 \cdot 10^{-3}\ s^{-1}$ and $6 \cdot 10^{-3}\ s^{-1}$ for the Fab dimers formed by the flexible divalent haptens N^{α},N^{ϵ}-di(dinitrophenyl)-L-lysine (Γ = 16 Å) and bis(N^{β}-2,4-dinitrophenyl-alanyl)-*meso*-diamino-succinate (Γ = 21 Å). Making the simplifying assumption that a single step binding equilibrium prevails, the corresponding dimer formation rate constants were calculated to be $1.9 \cdot 10^{5}\ M^{-1}\ s^{-1}$ and $1.1 \cdot 10^{4}\ M^{-1}\ s^{-1}$, respectively. In contrast, all haptens with spacers longer than 40 Å (i.e., bis(N^{α}-2,4-dinitrophenyl-tri-D-alanyl)-1,7-diamino-heptane, and di(N^{ϵ}-2,4-dinitrophenyl)-6-aminohexanoate-aspartyl-(prolyl)$_n$-L-lysyl (n = 24, 27, 33) exhibit a relative fast dimerization rate of the Fab fragments ($>7 \cdot 10^{6}\ M^{-1}\ s^{-1}$). These observations were interpreted as being caused by orientational constraints set by the limited solid angle of the reaction between the macromolecular reactants. Thus, ligands having better access to the binding site would react faster.

INTRODUCTION

Clustering of two or more IgE-molecules bound to the monovalent type I Fc_{ϵ} receptor ($Fc_{\epsilon}RI$) on mast cells or basophils is the initial step in the biochemical cascade finally leading to the secretory response of these cells (Siraganian et al., 1975; Segal et al., 1977; Metzger, 1977; Barsumian et al., 1981; Balakrishnan et al., 1982; Ishizaka and Ishizaka, 1984; Ortega et al., 1988). Understanding the physical and structural requirements that determine the extent of the cellular response to the produced oligomers are still in their emergence. One approach to investigating the properties of oligomers formed upon the interaction between multivalent antigens and the divalent IgE molecules has been using well defined, divalent haptens. Indeed, divalent haptens with spacers of different length and flexibility have been employed to study the relation between the extent of IgE oligomerization and the mediator release by mast cells and basophils (Siraganian et al., 1975; Dembo and Goldstein, 1978*a*, 1978*b*; Dembo et al., 1978, 1979*a*, 1979*b*; Goldstein et al., 1979). These studies have, however, been carried out using polyclonal IgE antibodies and hence the oligomerization process was less amenable to a quantitative analysis. Recently, Erickson et al. (1986) investigated the binding of mono- and divalent DNP haptens to the monoclonal, DNP-specific IgE produced by the hybridoma H1 26.82 (Liu et al., 1980). These IgE were covalently labeled with fluorescein-5-isothiocyanate (FITC) and the emission of the FITC-IgE was found to undergo quenching upon DNP binding. From these fluorescence titrations, Erickson et al. (1986) deduced that the short and flexible divalent hapten bis[(N^{ϵ}-2,4-dinitrophenyl)amino]caproyl]-L-tyrosyl]cystine ((DCT)$_2$-cystine) caused formation of IgE dimers, both in solution and on the surface of mucosal mast cells (line RBL-2H3). However, no further characterization and discrimination between open and closed oligomers of different size was done. More recently, Schweitzer-Stenner et al. (1987) studied the binding equilibrium of divalent haptens to the monoclonal, DNP-specific IgE antibodies produced by the hybridoma A2 (Rudolph et al., 1981). The different titrations were analysed by applying the thermodynamic model of Dembo and Goldstein (1978*a*). It was found that all divalent haptens with spacer lengths between Γ = 15–130 Å caused the formation of closed ring dimers. Furthermore, the oligomer formation or the corresponding ring closure was found to proceed on a time scale of several minutes. This is rather slow compared with the

Abbreviations used in this paper: NET, nonequilibrium titration; DNP, 2,4 dinitrophenyl; Ahx, 6-aminohexanoate; But, -γ-aminobutyric acid; Asp, L-aspartate; (Pro)$_n$, polypeptide containing n L-prolines; di(DNP)-lys, N^{α},N^{ϵ}-di(dinitrophenyl)-L-lysine; bis(DNP-ala), bis(N^{β}-2,4-dinitrophenyl-alanyl)-*meso*-diamino-succinate bis(DNP-tri-D-Ala), bis(N^{α}-2,4-dinitrophenyl-tri-D-alanyl)1,7-diamino-heptane; bis(DNP)-(pro)$_n$, di(N^{ϵ}-2,4-dinitrophenyl)-6-aminohexanoate-L-aspartate-(prolyl)$_n$-lysyl; (DCT)$_2$-cystine, bis[[[(N^{ϵ}-2,4-dinitrophenyl)amino]caproyl]-L-tyrosyl]cystine; RMS, root mean square.

0006-3495/92/08/551/12 $2.00

association and dissociation rates observed for antibody interactions with monovalent haptens (cf. Haselkorn et al., 1974; Lancet and Pecht, 1977).

Erickson et al. (1987) and Goldstein et al. (1989) also reported kinetic measurements of the interactions between monovalent DNP haptens and monoclonal DNP-specific IgE-H1-26.82 in solution and on the surface of RBL cells. Moreover, Posner et al. (1991) investigated the dissociation of the divalent hapten $(DTC)_2$-cystine from IgE-H1-26.82 in solution. Their results suggest that the dimers formed upon reaction of these reagents dissociate quite slowly, i.e., on a time scale 10^2–10^3 s. However, because only intact IgE was used in the latter study, discrimination between open dimers and ring closure was not possible.

In this study, we performed fluorescence titrations of the Fab fragments of the murine, DNP-specific IgE-A2 by divalent DNP haptens at variable rates of hapten addition. The measurements carried out with hapten addition rates faster than a distinct threshold value yielded titrations reflecting a nonequilibrium state of the hapten-Fab reaction (NET: nonequilibrium titration). Hence, they provide information about its kinetics that can be derived by analyzing the data in terms of an appropriate theory. This approach yields the rates of the formation of Fab dimers, which can be regarded as models for the open dimers of the corresponding intact IgE. We used divalent haptens with short and flexible spacers, i.e., N^{α},N^{ϵ}-1,4-di(dinitrophenyl)-L-lysine (Γ = 16 Å), bis(N^{β}-2,4-dinitrophenyl-alanyl)-*meso*-diamino-succinate (Γ = 21 Å), with long and flexible spacers, i.e., bis(N^{α}-2,4-dinitrophenyl-tri-D-alanyl)-1,7-diamino-heptane and with long and rigid spacers, i.e., di(N^{α}-2,4-dinitrophenyl)-6-aminohexanoate-aspartyl-(prolyl)$_n$-lysyl (n = 24, 27, 33; Γ = 110–130 Å).

The latter haptens were also employed in NETs of intact IgE-A2-antibodies. This is the subject of the following paper.

MATERIALS AND METHODS

DNP-specific IgE-A2 antibody and its Fab fragments

The hybridoma cell line secreting the DNP-specific monoclonal IgE-A2 was obtained from the ATCC (Rudolph et al., 1981). Cells were first grown in tissue culture and later injected intraperitoneally into mice (Balb/c × C57B1/6)F_1 for propagation into ascites. The IgE antibodies were first absorbed on a N^{ϵ}-DNP-lysyl-Sepharose 4B (Pharmacia, Sweden) affinity column, and then the antibodies were eluted with two column volumes of 0.1 M dinitrophenolate solution in borate-buffered saline (0.2 M sodium borate, pH 7.4; 0.15 M NaCl) and dialyzed extensively against the same buffer. Residual dinitrophenolate was removed by passage through a Dowex 1.8, 100–200 mesh (BDH, UK) column (0.6 × 4 cm) in a solution consisting of 0.1 M NaCl and 0.01 M sodium phosphate buffer adjusted to pH 5.7. Finally, the antibodies were dialyzed extensively against 0.15 mM NaCl, 0.2 M sodium borate buffer of pH 7.4.

In order to produce Fab fragments of the thus obtained antibodies, 9.5 mg/2 ml IgE was dialyzed against 0.1 M Na acetate, pH = 5.5, 3 mM EDTA, then cystein was added to a final concentration of 10 mM. 2% activated papain (incubated with 50 mM cystein, 3 mM EDTA in the same buffer at 37°C) was added to start the digestion that proceeded for 14 h. After another portion of the enzyme was added, the incubation proceeded for another 3 h and the pH value was adjusted to 8.0. Subsequently, 2 mM DTT was added to reduce residual Fab_2 inter-heavy chains. Then, 50 mM iodoacetamide was added to alkylate the enzymes cystein, and the resulting fragments. Both reactions were allowed to proceed for 1 h at 37°C. Fractionation of the digest by passing through a Sephacryl S-300 (Pharmacia, Sweden) column (1 × 58 cm) yielded an elution profile with two peaks determined by measuring the absorption at 280 nm. Their analysis by SDS-PAGE without ME revealed that peak 2 is composed of the small peptides of the digested Fc portion of the IgE and of iodoacetamide, whereas peak 1 contained only one protein band that could be assigned to Fab fragments.

The concentration of the Fab in the sample was determined by measuring the light absorption at 280 nm using an OD_{280} = 1.62 (Liu et al., 1980) for a Fab concentration of 1 g/liter and an optical path length of 1 cm.

Preparation of the ligands

The monovalent N^{α}-2,4-dinitrophenyl-glycin (DNP-gly), N^{γ}2,4-dinitrophenyl-aminobutyric acid (DNP-but), N^{ϵ}-dinitrophenyl-aminocaproic-acid (DNP-cap), and the divalent N^{α},N^{ϵ},di(2,4-dinitrophenyl)-L-lysine (di(DNP-lys) haptens were obtained commercially from Sigma Chemical Co. (St. Louis, MO) and used without further purification. The divalent hapten bis(N^{β}-dinitrophenyl-alanyl)-*meso*-diamino-succinate (bis(DNP)-ala) was a kind gift of Dr. Verne Schumaker (UCLA). Its preparation and purification are described by Wilder et al. (1975). Bis(N^{α}-2,4-dinitrophenyl-tri-D-alanyl)-1,7-diamino-heptane (bis(DNP-tri-ala)) was synthesized and purified as described elsewhere (Schweitzer-Stenner et al., 1987). The long and rigid haptens N^{ϵ}-2,4-dinitrophenyl-6-aminohexanoate-L-aspartyl-(prolyl)$_{21}$-OH (DNP-(pro)$_{21}$) and di(N^{ϵ}-2,4-dinitrophenyl)-aminohexanoate-L-aspartyl-(proline)$_n$-lysyl with n = 24, 27, 33; (bis(DNP-(pro)$_n$) were synthesized by Dr. Immanuel Lüscher (Schweitzer-Stenner et al., 1987). The concentration of the DNP stock solutions were determined by absorption measurements using the following molar extinction coefficients: $\epsilon(\text{DNP-gly})_{364\,nm}$ = $1.78 \cdot 10^4$ M^{-1} cm^{-1}, $\epsilon(\text{DNP-cap})_{364\,nm}$ = $1.77 \cdot 10^4$ M^{-1} cm^{-1}, $\epsilon(\text{DNP-but})_{364\,nm}$ = $1.82 \cdot 10^4$ M^{-1} cm^{-1}, $\epsilon(\text{di-DNP-lys})_{364\,nm}$ = $\epsilon(\text{bis-DNP-ala})_{364\,nm}$ = $\epsilon(\text{bis-DNP-tri-ala})_{364\,nm}$ = $\epsilon(\text{bis-DNP-(pro)}_n)_{364\,nm}$ = $1.8 \cdot 10^4$ M^{-1} cm^{-1} (Wilder et al., 1975).

Fluorescence titrations

Hapten titrations of an Fab/IgE-solution

Hapten binding to the Fab fragments was measured in the following way: the hapten solution was added by a motor-driven syringe, at constant rate r_H to a protein solution contained in a spectrofluorometer cuvette. This rate is given by:

$$r_H = [H]_s \delta V_s / \delta t, \qquad (1)$$

where $[H]_s$ is the concentration of the titrants stock solution and δV_s is the volume of the stock solution added to the titrated solution in the time interval δt. The reactants were continuously mixed by a mechanical stirrer and the temperature was kept constant at 37°C. The titration rate was adjusted by changing the speed of the driving motor and/or the volume of the syringe. The total hapten concentration $[H]_T$ of the sample is linearly related to the titration time t given by:

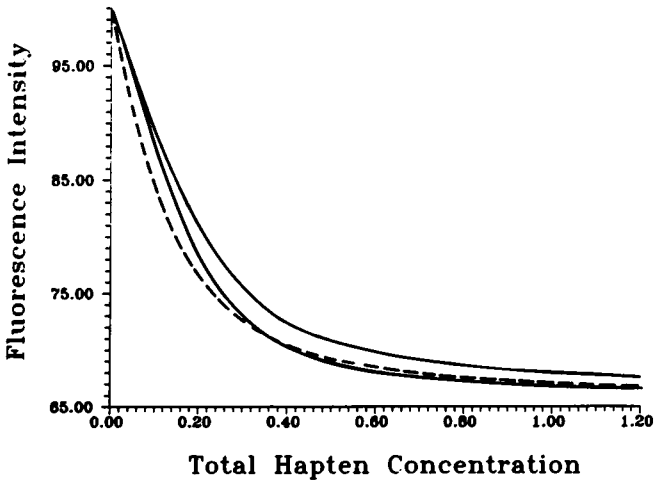

FIGURE 1 Schematic representation of the fluorescence titration curves resulting from different hapten addition rates r_H. The dashed titration curve was observed at $r_H < r_H^*$ and therefore represents the equilibrium of the monitored binding process. The NET represented by the solid lines are the results of measurements with two different hapten addition rates faster than r_H^*. The upper curve results from the faster r_H. The total hapten concentration is expressed in units of 10^{-6} M.

$$[H]_t = \frac{[H]_s \cdot r_H \cdot t}{(V_0 + r_H \cdot t/[H]_s)}, \quad (2)$$

where V_0 is the initial volume of the protein sample and t is the titration time. Since the volume of the protein sample changes during the titration, we have corrected the Fab concentration for dilution using the equation:

$$[\text{Fab}]_T = [\text{Fab}]_{T0} V_0/(V_0 + t\delta V_s/\delta t), \quad (3)$$

where $[\text{Fab}]_{T0}$ is the initial Fab concentrations of the sample. $[\text{Fab}]_T$ denotes the total Fab concentration at the titration time t.

Monitoring of hapten binding

DNP-hapten binding to the Fab-combining site causes a nonradiative energy transfer mainly from the intrinsic tryptophans to the bound DNP-group (Green, 1964). Therefore, hapten binding can be monitored by measuring the protein emission at 330 nm (excitation wavelength 280 nm) as a function of the titration time. The measured fluorescence intensity $I_0(t)$ was corrected for the effect of dilution by:

$$I(t) = I_0(t)(V_0 + t\delta V_s/\delta t)/V_0, \quad (4)$$

thus yielding the corrected value $I(t)$. Further correction for light absorption by the DNP-haptens (inner filter effect) was done by titrating an immunoglobulin with unrelated specificity (e.g., HOPC-8 or MOPC-104E) with the respective employed haptens. The final expression for the emission intensity, denoted I_c, is given by:

$$I_c(t) = I(t)I(t = 0)/I_{nsb}(t), \quad (5)$$

where $I_{nsb}(t)$ is the emission intensity monitored in the nonspecific titration and $I(t = 0)$ is the initial intensity. The experimental data were collected and digitized by a microcomputer (1,020 data points for each titration).

Protocol of the kinetic experiments

Fluorescence titrations carried out at rates of hapten addition larger than a distinct threshold value r_H^* become r_H dependent and reflect a nonequilibrium state of the hapten-Fab interaction. In order to illustrate the influence of r_H on the fluorescence titration, the solid lines in Fig. 1 display two NETs measured at different rates r_H. Their slopes have been derived by spline functions fitted to a data set observed with bis(DNP-β-ala). The upper curve herein monitors the NET measured with larger r_H. The dashed line displays the corresponding equilibrium titration measured at $r_H < r_H^*$. Increasing r_H yields a reduction of the fluorescence quenching, especially in the initial phase of the titration owing to the reduced number of occupied binding sites and the slightly lower tryptophan quenching in the monomeric Fab-hapten complex. At larger r_H, the NET intersects the equilibrium titration. As will be shown in the Results section, this is caused by the slow dissociation of the Fab dimers. The threshold value r_H^* depends on the total hapten and Fab concentrations and on the rate constants of the various reaction steps. Thus, it is not constant during the titration process. Its determination requires some preliminary experiments with each of the employed haptens. The kinetic parameters of the hapten-Fab interaction were derived from a set of NETs performed at different rates $r_H > r_H^*$. To ascertain that complete mixing of reactants in the sample is maintained throughout the titration, the time interval between two data points was always longer than 0.5 s. Hence, only processes with time constants smaller than 2 s^{-1} could be resolved.

THEORETICAL METHODS

Interaction between divalent haptens and Fab fragments

Here, we first describe a model of Fab-(divalent) hapten interaction based on the assumption that the Fab dimer formation proceeds considerably slower than the corresponding binding of a monovalent hapten to the Fab combining sites (which holds for haptens with short and flexible spacers; cf. Result section). Thus, the model assumes that the time course of dimer formation is independent of the association and dissociation rates of the initial binding step. This yields a formalism that was fitted to the corresponding NETs (i.e., $r_H > r_H^*$) in order to derive the specific rates of dimer formation and dissociation.

Our kinetic model is based on the simplifying assumption that the Fab dimerization proceeds by a single binding step, i.e., possible conformational transitions within the Fab-dimer are neglected.

Formation of Fab-dimers

Fig. 2 illustrates the different steps considered in the analysis of the interactions between the divalent haptens and monovalent Fab fragments. The first step of the reaction is the binding of a divalent hapten to a Fab-combining site:

$$\text{Fab} + \text{H} \overset{2K_{int}}{\rightleftharpoons} \text{Fab-H}.$$

The equilibrium constant K_{int} defines the intrinsic affinity of one hapten of the divalent agent to the Fab. The second step is then the reaction of a free Fab fragment with the above divalent hapten-Fab complex to form a Fab dimer.

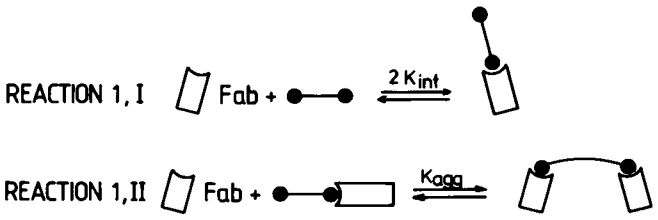

FIGURE 2 Scheme of the reaction between Fab fragments and divalent haptens. K_{int} is the intrinsic binding constant and K_{agg} is the equilibrium constant of the dimerization process.

$$\text{Fab-H} + \text{Fab} \overset{K_{agg}}{\rightleftarrows} (\text{Fab})_2\text{-H}.$$

We express the molar fractions X_{Me} and X_{De} of Fab-binding sites incorporated in monomers and dimers, respectively, using the mass action law:

$$X_{Me} = 2\,K_{int}[H]_{fe}[Fab]_{fe}/[Fab]_T \quad (6)$$

$$X_{De} = 4\,K_{int}K_{agg}[H]_{fe}[Fab]_{fe}^2/[Fab]_T \quad (7)$$

where $[H]_{fe}$ and $[Fab]_{fe}$ denote the equilibrium concentrations of free haptens and Fabs, respectively. We related these quantities to the total Fab and hapten concentrations ($[Fab]_T$, $[H]_T$), by using the law of mass conservation:

$$[H]_T = [H]_{fe} + 2\,K_{int}[H]_{fe}[Fab]_{fe} + 2\,K_{int}\,K_{agg}[H]_{fe}[Fab]_{fe}^2 \quad (8)$$

$$[Fab]_T = [Fab]_{fe} + 2\,K_{int}[H]_{fe}[Fab]_{fe} + 4\,K_{int}K_{agg}[H]_{fe}[Fab]_{fe}^2. \quad (9)$$

Eqs. 8 and 9 were solved simultaneously for $[H]_{fe}$ and $[Fab]_{fe}$ by means of a two-dimensional version of the Newton-Raphson method (Margenau and Murphy, 1956) in a zero-search routine.

The observed quenching of the Fab emission is proportional to the number of occupied binding sites. Thus the fluorescence intensity (Eq. 5) is given by:

$$I_c([H]_T) = I_{max}[1 - q_1X_{Me} - q_2X_{De}] \quad (10)$$

I_{max} is the initial intensity observed at $[H]_T = 0$. The quenching coefficient q_j is defined by:

$$q_j = (I_{max} - I_{min,j})/I_{max}, \quad (11)$$

where $I_{min,j}$ denotes the intensity of the quenched emission, which can be different for the occupied binding site of a monomer ($j = 1$) and a dimer ($j = 2$) (Schweitzer-Stenner et al., 1987).

Kinetics of Fab dimerization

We treated the kinetics by dividing each titration time T into N δt intervals (N is the number of digitized data points). All intervals were longer than 0.5 s. Thus, only processes with rates slower than 2 s^{-1} would affect the shape of the titration curve. To calculate the mole fraction of dimers formed at the end of each time interval δt, we solved the differential equation describing the dimerization process, i.e.:

$$d[D](t)/dt = -k_{agg}^-[D](t) + k_{agg}^+[M](t)[Fab]_f(t), \quad (12)$$

where k_{agg}^+ and k_{agg}^- denote the association and dissociation rate constants, respectively. $[M](t)$ and $[D](t)$ are the concentrations of monomeric and dimeric Fab-hapten complexes. $[Fab]_f(t)$ is the concentration of free Fabs. Since both literature data and titration experiments with monovalent DNP-haptens provide evidence that the first binding step proceeds significantly faster than the dimer formation monitored by NETs (cf. Experimental section; and Lancet and Pecht, 1977), we assumed that the corresponding species are in equilibrium at any time of the titration process. Hence, $[D](t)$ can be expressed in terms of the free hapten and Fab concentrations using the mass action law:

$$d[D](t)/dt = -k_{agg}^-[D](t) + 2\,K_{int}k_{agg}^+[H]_f(t)[Fab]_f^2(t). \quad (13)$$

$[H]_f(t)$ (i.e., concentration of free haptens) and $[Fab]_f(t)$ can be expressed in terms of the dimer concentration $[D](t)$ by using again the law of mass conservation:

$$[H]_f(t) = \alpha + \sqrt{\{\alpha^2 - \beta\}} \quad (14)$$

$$[Fab]_f(t) = [Fab]_T - [H]_T + [H]_f(t) - [D](t), \quad (15)$$

where

$$\alpha = \{[Fab]_T - [H](t) - [D](t) + (2K_{int})^{-1}\}/2$$

$$\beta = 1/2([D](t) - [H]_T)K_{int}^{-1}.$$

Eq. 13 was solved by the following iterative procedure: for the first iteration step we assumed that the free hapten and Fab concentrations do not change upon dimer formation. Hence, as a first guess the concentration of dimers formed at the end of each interval δt can be expressed by:

$$[D]_1(t + \delta t) = 2K_{int}K_{agg}[H]_{f0}(t)[Fab]_{f0}(t)^2 \times \{1 - \exp(-k_{agg}^-\delta t)\} + [D]_0(t)\exp(-k_{agg}^-\delta t), \quad (16)$$

where $K_{agg} = k_{agg}^+/k_{agg}^-$. The initial free hapten concentration $[H]_{f0}(t)$ and Fab concentration $[Fab]_{f0}(t)$ were calculated in terms of the total hapten and Fab concentrations and the initial dimer concentration $[D]_0(t)$ using Eqs. 14 and 15. In a second step, we recalculated the concentration $[H]_{f1}(t + \delta t)$ and $[Fab]_{f1}(t + \delta t)$ by using the value $[D]_1(t + \delta t)$ in Eqs. 14 and 15. These values were then introduced into Eq. 16 and used to recalculate the dimer concentration yielding $[D]_2(t + \delta t)$. This was repeated until convergence was reached, i.e., $|[D]_i - [D]_{i-1}| < 0.01 * [D]_i$. It should be noted that even though only the dissociation rate constant appears in the exponential function of Eq. 16, the time constant of the dimer formation also depends on the association rate constant. This is due to the time dependence of the product $2\,K_{int}K_{agg}[H]_f\,[Fab]_f^2$, which varies the saturation level defined by Eq. 16. The mole fractions of Fab fragments incorporated into monomeric and dimeric complexes can now be expressed as:

$$X_M(t + \delta t) = 2\,K_{int}[H]_f(t + \delta t)[Fab]_f(t + \delta t)/[Fab]_T \quad (17)$$

$$X_D(t + \delta t) = 2[D](t + \delta t)/[Fab]_T. \quad (18)$$

To calculate the fluorescence titration curves, Eqs. 17 and 18 are inserted into Eq. 10.

Fitting procedure

The aggregation constant K_{agg}, the disaggregation rate constant k_{agg}^-, and the quenching coefficient q_j are used as free parameters in the fit to the NETs. Moreover, K_{agg} was independently derived from the fit to the corresponding equilibrium titration. In a first attempt, the data were fitted by use of K_{int} values derived from the titrations with appropriate monovalent haptens, i.e., DNP-but for bis(DNP-ala), DNP-cap for bis(DNP-tri-D-ala), and DNP-$(pro)_{21}$ for bis(DNP)-$(pro)_n$. The divalent hapten di(DNP)-lys is asymmetric: one DNP-group is bound at the N^ϵ and is expected to exhibit a K_{int} value similar to that found for DNP-but, whereas the second one is bound at the N^α in proximal to the carboxylate. Hence, its intrinsic binding constant should be approximately that of DNP-gly. Therefore, we used the average value of these two intrinsic affinities as an initial guess for the K_{int} value of di(DNP)-lys. Using thus determined K_{int} values for the employed divalent haptens in the fits to the corresponding NETs and equilibrium titrations, we obtained satisfactory reproduction of the data. Some fine tuning of the fits was provided by allowing the K_{int} value to vary in a small interval (factor 0.5–2) around the input value. For the fitting procedure we used a program called MINUITL obtained from the CERN library (James, 1972). It contains three different minimization subroutines, SEEK, SIMPLX, and MIGRAD designed to search a local minimum

TABLE 1 **Best fit parameter values derived from the titration of monovalent haptens and the Fab fragments of the A2-IgE antibodies**

Hapten	K_{int} [M^{-1}]	q
DNP-gly	$1.0 \cdot 10^5$	0.35
DNP-but	$5.2 \cdot 10^6$	0.31
DNP-cap	$8.5 \cdot 10^6$	0.35
DNP-ahx-asp-pro_{21}-OH	$1.2 \cdot 10^7$	0.32

The haptens employed are: DNP-gly, DNP-but, DNP-ahx, and DNP-$(pro)_{21}$.

in the corresponding χ^2 function. The model to be fitted is not linear. Hence, the standard deviations that can in principle be calculated from a parabolic approximation to the χ^2 function (i.e., a m + 1-dimensional hyperplane; m, number of parameters) near the minimum determined by the final parameter values do not represent the real statistical error. Correlation effects between the parameters cause additional uncertainties (Grinvald and Steinberg, 1974). In order to obtain real statistical errors, we employed the MINUITL subroutine CONTOUR, which calculates the projection of the χ^2 function on a two-dimensional subspace of the parameter space (Müller and Plesser, 1991). The respective hypercontours were plotted in terms of confidence levels defined by $\chi^2 = \chi^2_{min} + \delta$. For all our fits we used a $\delta = 4$. The corresponding probability to obtain parameter values in the limit of this confidence region is 70%. The maximal and the minimal parameter values of the confidence region were used to calculate a realistic statistical error of the respective parameters.

RESULTS

Titrations with monovalent haptens

To determine initial values for the intrinsic binding constants K_{int} of the employed divalent haptens to the Fabs, the monovalent haptens DNP-gly, DNP-but, DNP-ahx, and DNP-$(pro)_{21}$ were used for titrations of the Fab fragments. By titrating the Fab fragments at different hapten addition rates, practically identical titration curves were obtained (data not shown). This established that equilibrium was achieved irrespective of the hapten addition rate r_H and that the binding proceeds within times shorter than 0.5 s. Consequently, the titration curves could all be fitted to a model that describes the equilibrium of monovalent hapten binding to a Fab-site by a single-step reaction. All titrations could be fitted assuming that the binding activity of the Fabs was practically 100%.[1] The derived binding constants and the maximal values of fluorescence quenching (Table 1) were all consistent with those of earlier studies (Schweitzer-Stenner et al., 1987).

Titrations with divalent haptens

Whereas analysis of the monovalent haptens binding to the Fabs is a straightforward procedure, that of the divalent haptens required a distinct choice of experimental parameters, because multiple steps are involved in these interactions (see Theory section). The protocol that we adopted to attain appropriate experimental conditions (i.e., hapten addition rates, stock concentrations of the haptens, Fab concentrations), has already been described in detail earlier (Schweitzer-Stenner et al., 1987). The NETs of all the employed haptens and Fabs have been repeated at different rates $r_H > r_H^*$ as indicated in Table 2.

Figs. 3, *a* and *b* display two representative NETs where the titrations of the Fabs by short and flexible haptens (di(DNP)-lys and bis(DNP-ala)) were monitored at different hapten addition rates. The experimental data are displayed by a reduced number of points (i.e., 18 out of the original number of 1,200) for clarity. The marked dependence of these titration curves on the rate of hapten addition clearly contrasts with those of the monovalent haptens (data not shown) and suggests that the rate of dimerization is slower than the threshold of 0.5 s^{-1}. Consequently, these curves cannot be fitted using a theory that is based only on equilibrium of hapten-Fab interactions. The application of the kinetic model introduced above, however, does yield satisfactory fits to the NETs as judged by the solid lines in Fig. 3, *a* and *b*.

Table 2 summarizes the fitting parameters derived from the NETs. The disaggregation rate constants derived for the corresponding NETs are the same within the limits of accuracy. The aggregation constants K_{agg} turned out to be considerably larger than those derived from the respective titrations of the intact IgE (cf. Schweitzer-Stenner et al., 1987). This discrepancy is discussed below. The corresponding dimer formation rate constants k^+_{agg} are $1.9 \pm 0.6 \cdot 10^5$ M^{-1} s^{-1} and $1.7 \pm 0.6 \cdot 10^4$ M^{-1} s^{-1}, respectively. The maximal quenching values q_1 and q_2 differ slightly from each other. Eq. 18 was used to calculate the corresponding molar fraction of Fab-dimers as a function of the total hapten concentration. Results of these calculations are displayed in Fig. 4, which shows the extent of dimerization for a nonequilibrium and the equilibrium situation of the interaction between di(DNP)-lys and Fabs. From these plots it can be seen that the maximum of dimer formation is shifted towards higher hapten concentrations upon decreasing the hapten addition rate. This shows that at high total hapten concentrations the NETs reflect a larger extent of dimerization than the corresponding equilibrium binding curves owing to the slow disaggregation of the Fab dimers. At very fast hapten addition rates this can cause an intersection of the NET and equilibrium titration as shown in Fig. 1.

In contrast to these findings, the titration with bis(DNP-tri-ala) (Fig. 3 *c*) and with bis(DNP)-$(pro)_{33}$ (Fig. 3 *d*) does not depend on the hapten addition rate. The same holds for the titrations by the other divalent haptens with oligoproline spacers (n = 24, 27; data not

[1] This is in contrast to what has been obtained for hapten binding to the DNP-specific IgE-H1 26.82 (Kubitscheck et al., 1991).

TABLE 2 **Best fit parameters of the titration of divalent DNP-haptens and the Fab fragments of DNP-specific, monoclonal A2-IgE at different experimental conditions, i.e., $[H]_S$, r_H, and $[Fab]_T$**

r_H [mol/s]	H_S [M]	$[Fab]_T$ [M]	K_{int} [$M^{-1} \cdot 10^6$]	K_{agg} [$M^{-1} \cdot 10^6$]	k^-_{agg} [$s^{-1} \cdot 10^{-3}$]	k^+_{agg} [$M^{-1} s^{-1} \cdot 10^5$]	q_M	q_D
I. di(DNP)-lys								
$5.0 \cdot 10^{-10}$	$7.3 \cdot 10^{-4}$	$5 \cdot 10^{-7}$	2.3 ± 0.3	25 ± 9	7.8 ± 6	1.9 ± 1.6	0.44	0.33
$1.0 \cdot 10^{-9}$	$7.3 \cdot 10^{-4}$	$5 \cdot 10^{-7}$	2.3 ± 0.3	25 ± 9	7.8 ± 6	1.9 ± 1.6	0.41	0.37
II. bis(DNP-ala)								
$5.5 \cdot 10^{-10}$	$8.0 \cdot 10^{-5}$	$2.5 \cdot 10^{-7}$	5.0 ± 0.5	2.8 ± 0.8	4.7 ± 2.0	0.13 ± 0.04	0.34	0.52
$7.0 \cdot 10^{-10}$	$1.0 \cdot 10^{-4}$	$2.5 \cdot 10^{-7}$	5.0 ± 0.5	2.8 ± 0.8	6.3 ± 2.0	0.17 ± 0.06	0.35	0.47
$1.4 \cdot 10^{-9}$	$1.0 \cdot 10^{-4}$	$2.5 \cdot 10^{-7}$	5.0 ± 0.5	2.8 ± 0.8	6.2 ± 2.0	0.17 ± 0.06	0.34	0.44
$5.8 \cdot 10^{-9}$	$1.0 \cdot 10^{-4}$	$2.5 \cdot 10^{-7}$	5.0 ± 0.5	2.8 ± 0.8	12.0 ± 4.0	0.34 ± 0.14	0.33	0.43
III. bis(DNP-tri-ala)								
$1.4 \cdot 10^{-10}$	$1.0 \cdot 10^{-5}$	$2.5 \cdot 10^{-7}$	8.5 ± 0.5	4.2 ± 1.5	$>10^3$	>70	0.31	0.41
$2.8 \cdot 10^{-10}$	$1.0 \cdot 10^{-5}$	$2.5 \cdot 10^{-7}$	8.5 ± 0.5	4.2 ± 1.5	$>10^3$	>70	0.31	0.43
$5.6 \cdot 10^{-10}$	$1.0 \cdot 10^{-5}$	$2.5 \cdot 10^{-7}$	8.5 ± 0.5	4.2 ± 1.5	$>10^3$	>70	0.31	0.45
IV. bis(DNP)-$(pro)_{33}$								
$1.6 \cdot 10^{-10}$	$5.9 \cdot 10^{-6}$	$1.25 \cdot 10^{-7}$	9.0 ± 1.0	3.3 ± 0.8	$>10^3$	>70	0.33	0.33
$4.0 \cdot 10^{-10}$	$5.9 \cdot 10^{-4}$	$1.25 \cdot 10^{-7}$	9.0 ± 1.0	2.4 ± 0.8	$>10^3$	>70	0.32	0.32

shown). Consequently, all these can be fitted in terms of an equilibrium model for the hapten-Fab reaction. The respective rate constants of dimer formation are apparently larger than 2 s^{-1}. The values derived for the aggregation constant K_{agg} (Table 2) are in agreement with the results of corresponding titrations with intact IgE (cf. Schweitzer-Stenner et al., 1987). All NETs and equilibrium titrations could be fitted assuming that the ligand binding capacity is 100%.

Error analysis

A special subroutine of the fitting routine MINUITL was used to calculate the hypercontours of a two-dimensional subspace in order to elucidate the real statistical errors in the observed parameter values. The results of these calculations are given in Table 2.

As an example, the hypercontours of the parameters of the titration of the Fab fragments by bis(DNP-ala) are displayed in Fig. 5. The hatched area indicates the 70% confidence region. The statistical errors are provided by the lateral lengths of a rectangle which frames the confidence region. As indicated in Fig. 5, the statistical errors of the aggregation constant K_{agg} and the dissociation rate constant k^-_{agg} are considerably larger due to correlation effects coupling K_{agg}, k^-_{agg}, and the quenching coefficient q_2. Such correlation effects are reflected by a pronounced elliptical shape of the confidence region. The statistical errors in the aggregation and dissociation rate constants are $\pm 0.8 \cdot 10^6$ M^{-1} ($\hat{=}$ 24%) and $1.8 \cdot 10^{-3}$ s^{-1} ($\hat{=}$ 34%), respectively. The statistical error in the dimeric quenching factor q_2 is ±0.025 ($\hat{=}$ 5%). Similar correlation effects were established for the fits to all other titration curves.

DISCUSSION

Preliminary measurements of the interaction between intact A2-IgE and divalent haptens revealed that it involves at least one relatively slow step that proceeds on a time scale of several minutes (Schweitzer-Stenner et al., 1987). Some of the kinetic aspects of this reaction were now investigated by fluorescence titrations using various hapten addition rates. In order to resolve among the distinct steps of divalent hapten-IgE interaction we first investigated the intrinsic binding of monovalent haptens to Fab fragments of IgE. The interactions between monovalent haptens and monoclonal antibodies have earlier been shown to be quite fast for all haptens employed (Haselkorn et al., 1974; Lancet and Pecht, 1977; Zidovetzki et al., 1980). The dissociation rate constants were usually found to be larger than 2 s^{-1}, and, hence, if a single step mechanism is assumed, the corresponding association rate constants would be higher than 10^7 M^{-1} s^{-1} (Table 1). The binding of divalent haptens to the Fab fragments of IgE yields a mixture of monomeric and dimeric complexes that can be regarded as simple models for the open dimers predominantly formed in the reaction of intact IgE with divalent haptens (cf. Schweitzer-Stenner et al., 1987). We found that divalent haptens with short spacers (Γ = 16–21 Å) cause a slow formation of Fab dimers (i.e., time constants between 10^{-2} s^{-1} and 10^{-3} s^{-1}), whereas those with longer spacers (Γ > 45 Å) effect a relatively fast dimerization with a time constant higher than 2 s^{-1}.

Thus, the NET is an effective tool for deriving the rate constants of slow processes that take place on a time scale of seconds and minutes. One may argue, however, that it would be more convenient to apply classical kinetic experiments to such processes, i.e., for example the measurements of the forward rate after mixing of the reactants. In our case, however, such an experimental protocol would not be appropriate for the following reasons. The first step of the (divalent) hapten-Fab interaction (i.e., the binding of the DNP-group to a Fab-site) has been shown to be fast even at low hapten concentra-

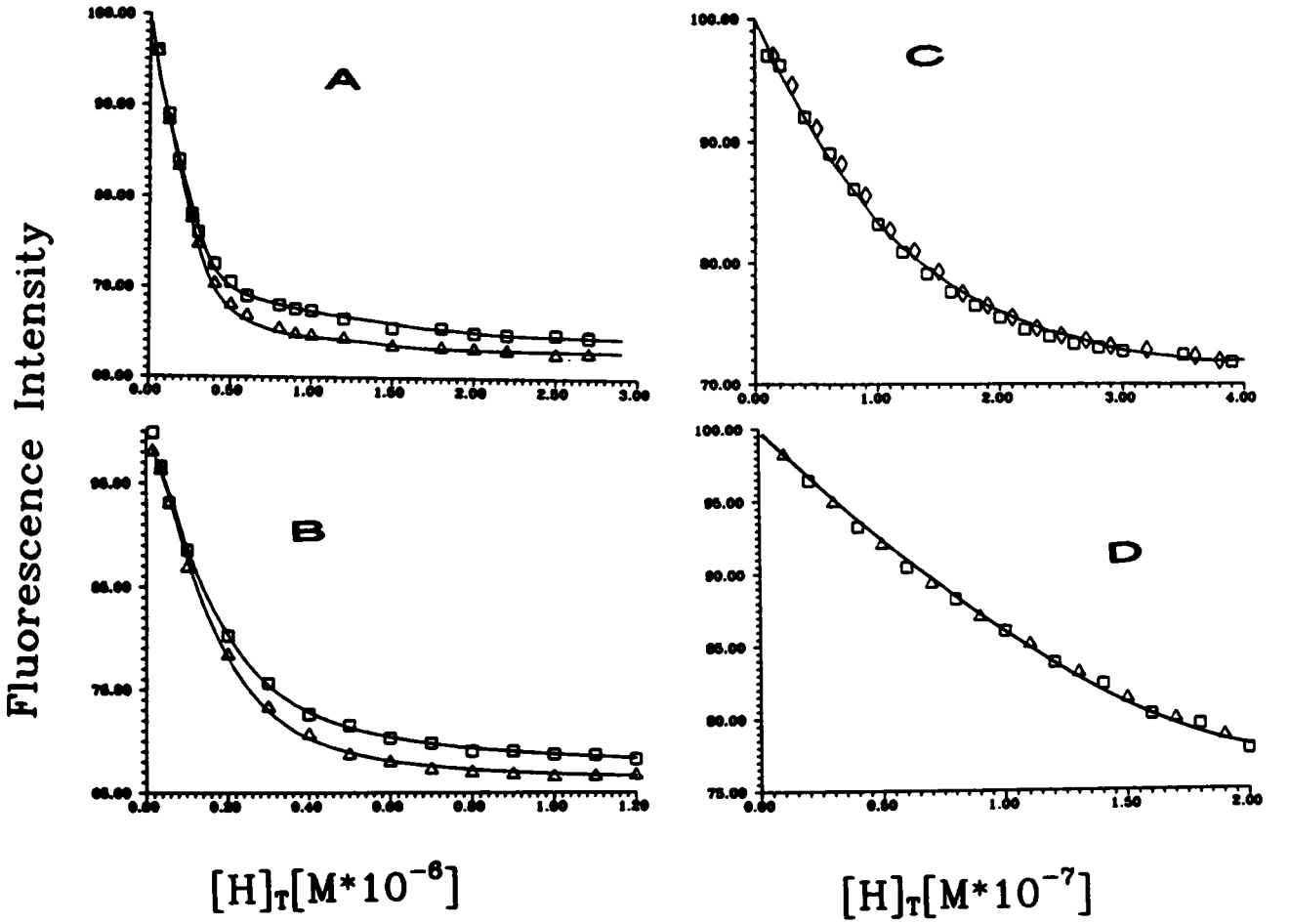

FIGURE 3 Fluorescence titrations of the Fab fragments with the divalent haptens di(DNP)-lys (*A*) ($r_H = 5.0 \cdot 10^{-10}$ mol/s (△) and $r_H = 1.0 \cdot 10^{-9}$ mol/s (□)), bis(DNP-ala) (*B*) ($r_H = 5.5 \cdot 10^{-10}$ mol/s (△) and $r_H = 1.4 \cdot 10^{-9}$ mol/s (□)), bis(DNP-tri-ala) (*C*) ($r_H = 1.4 \cdot 10^{-10}$ mol/s (◇) and $r_H = 5.6 \cdot 10^{-10}$ mol/s (□)) and bis(DNP)-pro_{33} (*D*) ($r_H = 1.6 \cdot 10^{-10}$ mol/s (△) and $r_H = 4.0 \cdot 10^{-10}$ mol/s (□)). The corresponding experimental parameters are given in Table 2. The representative data points (12 of 1,200) are taken from the smoothed fluorescence titration curves. The solid line is calculated using the best fit parameters given in Table 2.

tions. It would therefore require the use of rapid mixing techniques. The second reaction step, which is the principal subject of our investigation, causes only small changes of the intrinsic Fab fluorescence (cf. Fig. 1). Therefore, the difference between initial and final fluorescence intensity of the corresponding part of a forward rate curve is rather small, making a rigorous analysis difficult. Moreover, the derived parameters would have large statistical uncertainties. By using different NETs, however, the small additional fluorescence quenching caused by the Fab dimerization is continuously monitored at various ligand concentrations. Furthermore, performing the titrations at relatively slow rates of hapten addition allows the observation of the equilibrium of the reaction. Thus, the equilibrium constant K_{agg} can also be derived and compared with the ratio k^+_{agg}/k^-_{agg} obtained from the kinetic analysis of the corresponding NETs.

Unfortunately, we could not simply apply the elegant method proposed by Baird and co-workers (Goldstein et al., 1989; Posner et al., 1991; Erickson et al., 1991) to investigate the kinetics of hapten interactions with IgE-A2. Their technique is based on quenching of FITC-labeled IgE H1 26.82 by DNP binding. Such quenching is not observed, if one uses FITC-labeled IgE-A2 (Kubitscheck, 1990).

In the following we address two aspects of our results. First, we apply the reaction theory of Schmitz and Schurr (1972) in order to rationalize the slow aggregation and disaggregation of Fab complexes with divalent haptens of short and flexible spacers. Second, we discuss some discrepancies between the K_{agg} values of IgE- and Fab-dimerization observed with divalent haptens.

The influence of spatial constraints on the dimer formation rate

A bimolecular reaction can be described in terms of a two-step mechanism (Eigen, 1974; DeLisi, 1980). The first step is assigned to the formation of an encounter

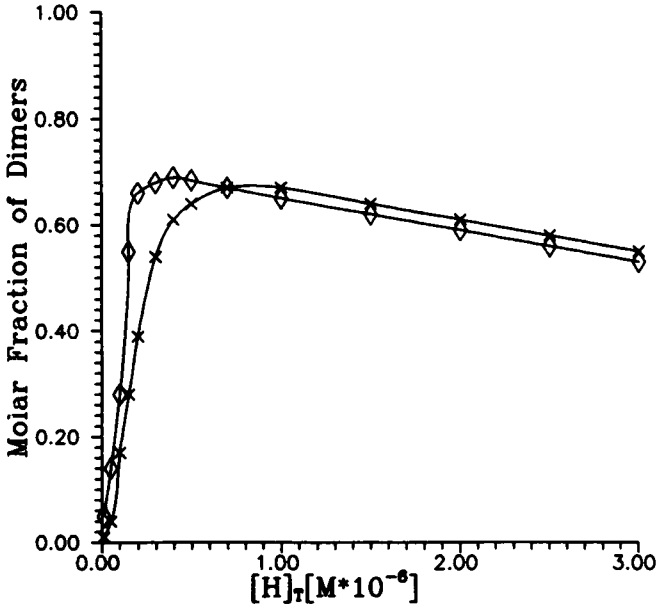

FIGURE 4 Plot of the molar fraction of Fab molecules incorporated into dimers upon reaction with di(DNP)-lys (results of NET (×), results of equilibrium titration (◇)).

complex (encounter step), whereas only the second yields the final product where the specific noncovalent contacts between the ligand (L) and its combining site (C) are formed. The formation of the encounter complex C--L is determined exclusively by the diffusion of the reactants, whereas the second reaction step is governed by the physical interaction between them:

$$C + L \underset{k_{21}}{\overset{k_{12}}{\rightleftarrows}} C\text{--}L \underset{k_{32}}{\overset{k_{23}}{\rightleftarrows}} C - L.$$

In the process of Fab dimerization, the monomeric Fab divalent hapten complex is considered as a ligand (L) that binds to the combining site C of a free Fab. Since the rate constant k_{23} in the above scheme is expected to be determined by the physical properties of the reactive sites of the ligand (i.e., DNP) and the Fab-combining site, k_{23} should be similar for first binding and dimerization steps. Thus, the difference between the fast association rates of the first binding step and the slow dimer formation rates k^+_{agg} should mainly reflect different diffusive association rate constants k_{12}.

If k^+_{agg} is controlled by diffusion, it should be in the order of $10^8\ M^{-1}\ s^{-1}$ (Posner et al., 1991). This is two to three orders of magnitude larger than the k^+_{agg} values found experimentally for the Fab dimerization by haptens with short spacers. This calculation of the diffusion rate constant, however, is based on a 4π solid angle for the reaction sphere of the dimer formation, which is valid for small molecules as reactants. However, if one of the reactants is a macromolecule, the active site of which occupies a rather small fraction of its surface area, the solid angle of the reactive site is significantly reduced. In the case of antibody-hapten reactions it is not larger than 2π (Lancet and Pecht, 1977). A further reduction in the solid angle may occur if both reactants are macromolecules (Dembo and Goldstein, 1978*b*; DeLisi, 1980). Fig. 6 schematically illustrates the reaction between a Fab-hapten complex and a free site on another Fab. The hatched rectangles are cross-sections of the two Fabs considered as symmetrical cylinders with a radius R_T. The divalent hapten is drawn as a thin stick with two small circles at its end representing the DNP groups. If the length R_H of the free part of the spacer, given by:

$$R_H = \Gamma - 2d, \tag{19}$$

is smaller than R_T (this situation is sketched in Fig. 6), the solid angle of the free binding site reaction is significantly smaller than 2π. Thus, the polar angle θ between the normal to the binding site and the Fab-hapten complex cannot be larger than a limiting value θ_0, because the movement of the upper Fab with respect to the lower is subject to steric hindrance. If, however, R_H is significantly larger than R_T, the Fabs do not interact with each other in the encounter complex. In this case the maximal polar angle is only determined by the size and the depth of the Fab-combining site.

Thus, the diffusive rate constant k_{12} now depends on two different processes: the lateral diffusion of the ligand into the reaction sphere, and its orientational diffusion leading to an appropriate polar angle θ smaller than θ_0. Since R_H is smaller than R_T for the dimerization processes caused by di(DNP)-lys and bis(DNP-ala), one suspects that their slow rates reflect the predominant influence of the orientational diffusion on the formation of the respective encounter complexes.

In order to test whether this hypothesis is physically justified, we estimated the influence of spatial constraints on k^+_{agg} by means of the reaction theory developed by Schmitz and Schurr (1972). It computes the apparent diffusion rate constant of a reaction as a function of the minimal polar angle θ_0.

Using the model of Schmitz and Schurr (1972), Shoup et al. (1981) presented an analytical solution of their steady-state rotational-translational diffusion equation based on the assumption that the flux of the ligand is constant over the reactive part of the free Fab. It expresses k_{12} in terms of Legendere polynomials $P_l(\cos\theta_0)$ by means of the following equation:

$$k^+_{12} = \frac{4\pi R_H^2 Dk(1-\cos\theta_0)^2 L}{4D_R(1-\cos\theta_0) + kR_H \sum_l \{(P_{l-1}(\cos\theta_0) - P_{l+1}(\cos\theta_0))^2/\Omega_l\}}, \tag{20}$$

where D_T is the translational diffusion coefficient and L is the Avogadro constant. The factor k is defined by:

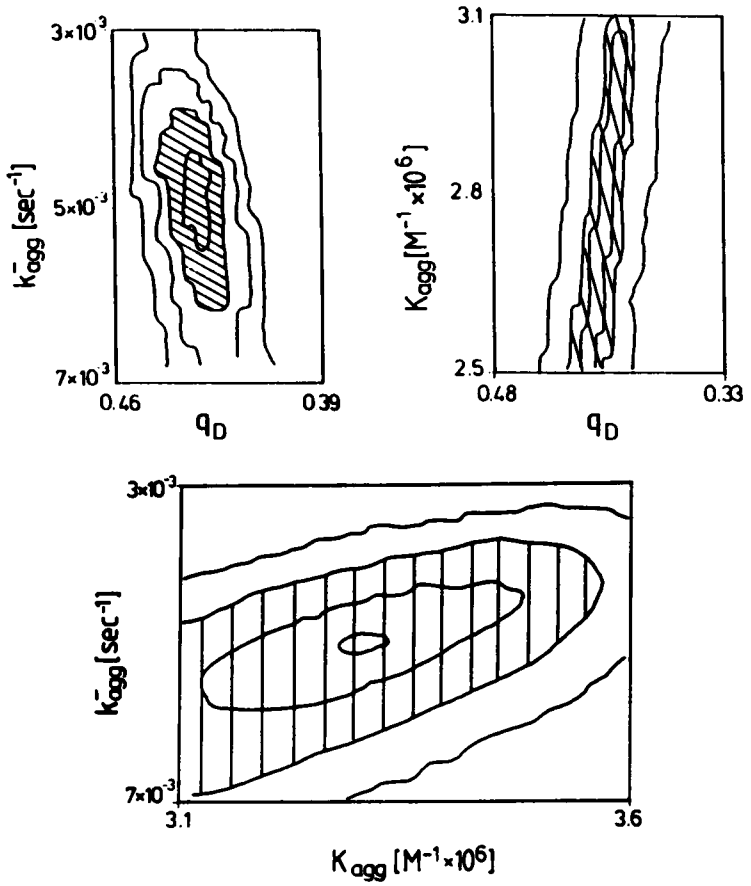

FIGURE 5 Plot of the hypercontours illustrating the two-dimensional parameter subspace of the fit to the titration curves of meso-bis[(N$^{\beta}$,DNP-β-Ala)amino]succinate. The cross-hatched area marks the confidence region of 70% probability for finding the corresponding parameter values.

$$k = 10R_T D_T / R_H^2. \quad (21)$$

The factor Ω_1 depends on the degree of the Legendre polynomial employed and is given by:

$$\Omega_1 = (1 + 1/2)(1 + R_H\sqrt{[1(1 + 1)D_R/D_T]}), \quad (22)$$

where D_R denotes the rotational diffusion coefficient. In order to calculate Ω_1 we use the Stokes-Einstein expressions for D_T and D_R, namely:

$$D_T = RT/6\eta R_T \quad (23)$$

$$D_R = RT/8\pi\eta R_T^3, \quad (24)$$

where η is the solvent viscosity, T the absolute temperature, and R the gas constant.

In order to estimate the influence of spatial constraints on the dimer formation by means of this theory we first calculated θ_0 as function of R_H for $R_H < 10$ Å by use of the equation (Fig. 6):

$$\theta_0 = \arctan(R_H/R_T). \quad (25)$$

Assuming the depth of the Fab-binding site to be 6 Å (Poljak, 1978) one estimates the corresponding R_H as 4 and 9 Å, respectively. These θ_0 values were inserted into Eq. 20. The corresponding k_{12} values are listed in Table 3. They reveal that for $R_H < 10$ Å spatial constraints reflected by decreasing θ_0 reduce the diffusion rate constant k_{12} from 10^8 M^{-1} s^{-1} (pure lateral diffusion) to 10^5–10^4 M^{-1} s^{-1} (restricted solid angle of the free Fab binding site with $\theta_0 < 0.5$ rad). These k_{12} values are qualitatively similar to the rate constants k_{agg}^+ of Fab dimerization by di(DNP)-lys and bis(DNP-ala). The R_H values of the other haptens are larger than 40 Å ($\gg R_T$). Hence, their diffusion rates are not affected significantly by orientational constraints in accordance with the experimental results.

Whereas the employed model qualitatively accounts for the decrease in the dimer formation rate, it fails to predict the correct absolute values of k_{agg}^+(di(DNP-lys) and k_{agg}^+(bis(DNP-ala)) (cf. Table 2). Since the spacer length of di(DNP)-lys is shorter than that of bis(DNP)-ala, one expects k_{agg}^+ of the former to be larger than that of the latter. This, however, is not the case. This discrepancy is most probably due to limitations of our model that ignores the flexibility and electrostatic properties of the spacers and possible protein–protein interaction. The possible influence of the latter is briefly discussed below.

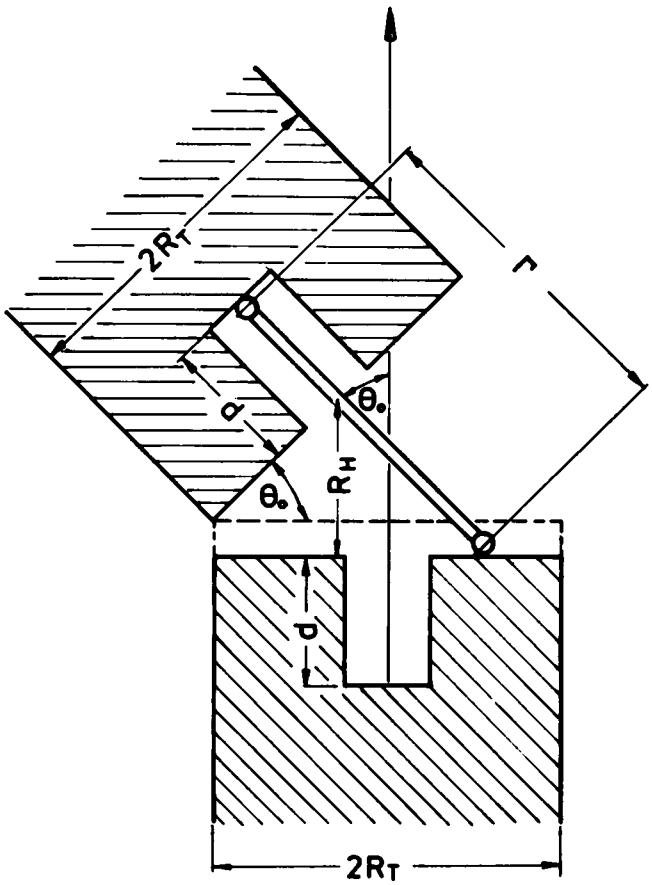

FIGURE 6 Schematic diagram of the encounter complex formed by an unligated Fab fragment and a hapten-Fab complex. The ligand is considered as a mobile sphere bearing a reactive site. The radius of this sphere is R_T. The binding site is a localized site on a plane. Its distance from the center of the reactive sphere is R_H. The orientation vector of the reactive site is tilted by the angle θ with respect to the normal vector of the binding site.

Comparison of the equilibrium constants of Fab- and IgE dimerization

The dimer formation equilibrium constants K_{agg} deserve some additional comments: the values determined for the interaction between the Fabs and the oligoproline haptens (Table 2) are nearly identical to those reported earlier (Schweitzer-Stenner et al., 1987) for the aggregation of intact IgE (note that the K_{agg} values reported in Table 1 of our earlier paper must be divided by two for comparison with the respective values in Table 2). The same holds for the corresponding results with bis(DNP-tri-ala). However, the K_{agg} value for the dimerization of the Fab fragment by bis(DNP-ala) is an order of magnitude larger than that of the aggregation of the intact IgE. An even larger difference between the K_{agg} values of Fab and IgE has been observed for di(DNP)-lys.

In order to explain these differences we have to recall that in our earlier paper (Schweitzer-Stenner et al., 1987) the thermodynamic model of Dembo and Goldstein (1978b) was employed to estimate the K_{agg} values for the IgE oligomer formation process. According to this model, K_{agg} decreases with decreasing spacer length. This procedure was employed to avoid correlation effects between K_{agg} and the ring closure constant J_2. In view of the K_{agg} values resulting from the analysis of the Fab dimerization, one may suppose that the model of Dembo and Goldstein (1979*b*) cannot be applied to analyzing results obtained with short and flexible haptens. In order to further clarify this point we refitted the fluorescence titrations with the haptens di(DNP)-lys and bis(DNP-ala). A detailed error analysis with the subroutine CONTOUR revealed large correlation effects coupling the parameters K_{agg} and the ring closure constant J_2. This especially holds for binding processes yielding a comparatively small amount of dimers (maximal, 20%). In this case the K_{agg} values resulting from the binding of bis(DNP-ala) can vary fivefold without reducing the quality of the fit or changing the calculated amount of formed dimers, if the equilibrium constant J_2 is lowered by nearly the same factor. Hence, it becomes apparent that, using the short haptens, larger K_{agg} values are possible for the IgE-oligomerization than those predicted by the model of Dembo and Goldstein (1978*b*).

It should be mentioned that interactions with the distinct DNPs of the asymmetric hapten di(DNP)-lys may yield slightly different K_{agg} values. Still, as one can learn from Eqs. 7 and 18, each of these constants is multiplied by the intrinsic binding constant K_{int} in the calculation of the molar fractions of occupied binding sites. This means that for asymmetric haptens the constant K_{agg} of side 1 is multiplied by the intrinsic constant K_{int} of side 2 and vice versa. Since each of these aggregation constants depends linearly on their respective intrinsic constant (i.e., $K_{agg}(1)$ depends on $K_{int}(1)$; Dembo and Goldstein, 1978b), the apparent products $K_{agg}K_{int}$ do not depend on the binding site. Therefore, the use of asymmetric haptens does not limit the applicability of the employed theory. The K_{agg} value for the cross-linking reaction by di(DNP)-lys must be regarded as an effective parameter

TABLE 3 Effect of spatial constraints on the diffusion rate constant of the formation of Fab dimers

R_H [Å]	θ_0 [rad]	k_1^+ [M^{-1} s^{-1}]	Hapten
2	0.1	$4.3 \cdot 10^3$	N^α, N^ϵ, di(DNP)-Lys
3	0.15	$1.3 \cdot 10^4$	
4	0.19	$3.1 \cdot 10^4$	
5	0.24	$5.8 \cdot 10^4$	
6	0.29	$9.7 \cdot 10^4$	
7	0.33	$1.5 \cdot 10^5$	*meso*-
8	0.38	$2.1 \cdot 10^5$	bis[(N^α, DNP-β-Ala)
9	0.42	$3.9 \cdot 10^5$	-amino] succinate

The constraints are parameterized by the maximal polar angle θ_0 restricting the solid angle of the reactive site for the binding of a Fab-hapten complex to a free Fab binding site.

averaging the contributions from the two different DNP environments of this hapten.

Finally, it is noteworthy, that K_{agg} of di(DNP)-lys is an order of magnitude larger than the corresponding intrinsic binding constant. This is a surprising result, because theoretical considerations (Dembo et al., 1978*b*) show that K_{agg} in solution should not exceed $K_{int}/2$. This can be rationalized, however, by assuming that the short spacer length of di(DNP)-lys brings the surfaces of two Fab-fragments close to the van der Waals contacts. Hence protein–protein interaction may stabilize this dimeric complex. This in turn may result in an increase of the corresponding equilibrium constant K_{agg}.

We conclude that the slow rate of Fab dimer formation as caused by the binding of short and flexible divalent haptens can be qualitatively understood in terms of orientational diffusion of the hapten Fab-complex into the solid angle of the reactive site of a free Fab. It is reasonable to assume that this also holds for the dimer formation between intact IgEs.

The authors are indebted to Professor Wolfgang Dreybrodt, Dr. Ulrich Kubitscheck, Dr. Ulrich Pilatus, and Diplom-Physiker Martin Kircheis for intensive, critical, and illuminating discussions. Furthermore, we would like to thank Mr. Gerd Ankele for drawing some of the figures.

The experimental part of this work was carried out when Reinhard Schweitzer-Stenner was a recipient of a short term MINERVA fellowship at The Weizmann Institute of Science. The generous support of the research reported in this paper by grants from the government of Lower Saxony, FRG, and The Tobacco Research Council USA Inc. is gratefully acknowledged.

Received for publication 16 August 1991 and in final form 26 March 1992.

REFERENCES

Balakrishnan, K., T. J. Hsu, A. D. Cooper, and H. M. McConnel. 1982. Lipid hapten containing membrane targets can trigger specific immunoglobulin E-dependent degranulation of rat basophilic leukemia cells. *J. Biol. Chem.* 257:6427–6433.

Barsumian, E. L., C. Isersky, M. G. Petrino, and R. Siraganian. 1981. IgE induces histamine release from rat basophilic leukemia cell lines. *Eur. J. Immunol.* 11:317–323.

DeLisi, C. 1980. The biophysics of ligand-receptor interactions. *Q. Rev. Biophys.* 13:201–230.

Dembo, M., and B. Goldstein. 1978*a*. Theory of equilibrium binding of symmetric bivalent haptens to cell surface antibody: application of histamine release from basophils. *J. Immunol.* 121:345–353.

Dembo, M., and B. Goldstein. 1978*b*. A thermodynamical model of binding of flexible bivalent haptens to antibody. *Immunochemistry.* 15:307–313.

Dembo, M., B. Goldstein, A. K. Sobotka, and L. M. Lichtenstein. 1978. Histamine release due to bivalent penicilloyl haptens: control by the number of cross-linked IgE antibodies on the basophil plasma membrane. *J. Immunol.* 121:354–358.

Dembo, M., B. Goldstein, A. K. Sobotka, and L. M. Lichtenstein. 1979*a*. Histamine release due to bivalent penicilloyl haptens: the relation of activation and desentization of basophils to dynamic aspects of ligand binding to cell surface antibody. *J. Immunol.* 122:5518–5528.

Dembo, M., B. Goldstein, A. K. Sobotka, and L. M. Lichtenstein. 1979*b*. Degranulation of human basophils: quantitative analysis of histamine release and desentization due to a bivalent penicilloyl hapten. *J. Immunol.* 123:1864–1872.

Eigen, M. 1974. Quantum Statistical Mechanics in Natural Sciences. S. L. Minz and S. M. Wiedermayer, editors. Plenum Press, New York. 37–61.

Erickson, J. W., P. Kane, B. Goldstein, D. Holowka, and B. Baird. 1986. Cross-linking of IgE-receptor complexes at the cell surface: a fluorescence method for studying the binding of monovalent and bivalent haptens to IgE. *Mol. Immunol.* 72:769–781.

Erickson, J. W., B. Goldstein, D. Holowka, and B. Baird. 1987. The effect of receptor density on the forward rate constant for binding of ligands to cell surface receptors. *Biophys. J.* 52:657–662.

Erickson, J. W., R. G. Posner, B. Goldstein, D. Holowka, and B. Baird. 1991. Bivalent ligand dissociation kinetics from receptor-bound immunoglobulin E: evidence for a time dependent increase in ligand rebinding at the cell surface. *Biochemistry.* 30:2357–2363.

Green, N. M. 1964. Avidin. 5. Quenching of fluorescence by dinitrophenyl groups. *J. Biochem.* 90:564–568.

Goldstein, B., M. Dembo, A. K. Sobotka, and L. M. Lichtenstein. 1979. Some invariant properties of IgE mediated basophil activation and desensitization. *J. Immunol.* 123:1873–1852.

Goldstein, B., R. G. Posner, D. C. Torney, J. Erickson, D. Holowka, and B. Baird. 1989. Competition between solution and cell surface receptors for ligand. Dissociation of hapten bound to surface antibody in the presence of solution antibody. *Biophys. J.* 56:955–966.

Grinvald, A., and I. Z. Steinberg. 1974. On the analysis of fluorescence decay kinetics by the method of least squares. *Anal. Biochem.* 59:583–598.

Haselkorn, D., S. Friedman, D. Givol, and I. Pecht. 1974. Kinetic mapping of the antibody combining site by chemical relaxation spectrometry. *Biochemistry.* 13:2210–2222.

Ishizaka, T., and K. Ishizaka. 1975. Cell surface IgE on human basophil granulocytes. *Ann. NY. Acad. Sci.* 254:462–475.

James, F. 1972. Function minimization. Proceedings of the 1972 Cern-Computing and Data-Processing School, Pertisau, Austria. 72–121.

Kubitscheck, U. 1990. Untersuchung des transmembranen Signals zur Auslösung der Degranulation bei RBL-2H3 Zellen durch Messung der Energieübertragung und Rotationsdiffusion. Doctoral Thesis, University of Bremen. 71 pp.

Kubitscheck, U., M. Kircheis, R. Schweitzer-Stenner, W. Dreybrodt, T. G. Jovin, and I. Pecht. 1991. Fluorescence resonance energy transfer on single living cells. Application to binding of monovalent haptens to cell bound immunoglobulin E. *Biophys. J.* 60:307–318.

Lancet, D., and I. Pecht. 1977. Chemical relaxation in Molecular Biology. I. Pecht and R. Rigler, editors. Springer-Verlag, New York. 306–338.

Liu, F. T., J. W. Bohn, E. L. Ferry, H. Yamamoto, C. A. Molinaro, L. A. Shermann, N. R. Klinman, and D. H. Katz. 1980. *J. Immunol.* 124:2728–2736.

Margenau, H., and G. M. Murphy. 1956. The Mathematics of Physics and Chemistry, Van Nostrand, New York. 245 pp.

Metzger, H. 1977. Receptors and Recognition. A. Series, P. Cuatrceasas, and M. F. Greaves, editors. Chapman and Hall Ltd., London. Vol. 4:75–102.

Müller, K.-H., and Th. Plesser. 1991. Variance reduction by simultaneous multi-exponential analysis of data sets from different experiments. *Eur. Biophys. J.* 19:231–240.

Ortega, E., R. Schweitzer-Stenner, and I. Pecht. 1988. Possible orientational constraints determine secretory signals induced by aggregation of IgE receptors on mast cells. *EMBO (Eur. Mol. Biol. Organ.) J.* 7:4101–4109.

Poljak, R. J. 1978. Correlation between three-dimensional structure and function of immunglobulins. *CRC Crit. Rev. Biochem.* 5:45–84.

Posner, R. G., J. W. Erickson, D. Holowka, B. Baird, and B. Goldstein. 1991. Dissociation kinetics of bivalent ligand-immunoglobulin E aggregates in solution. *Biochemistry.* 30:2348–2356.

Rudolph, A. K., P. D. Burrows, and M. R. Wahl. 1981. Thirteen hybridomas secreting hapten-specific immunoglobulin E from mice with Ig^a and Ig^b heavy chain haplotype. *Eur. J. Immunol.* 11:527–529.

Schmitz, K. S., and J. M. Schurr. 1972. The role of orientational constraints and rotational diffusion in bimolecular solution kinetics. *J. Phys. Chem.* 76:534–545.

Schweitzer-Stenner, R., A. Licht, I. Lüscher, and I. Pecht. 1987. Oligomerization and ring closure of immunglobulin E class antibodies by divalent haptens. *Biochemistry.* 26:3602–3612.

Segal, D. M., J. D. Taurog, and H. Metzger. 1977. Dimeric immunoglobulin E serves as a unit signal for mast cell degranulation. *Proc. Natl. Acad. Sci. USA.* 74:2993–2997.

Shoup, D., G. Lipari, and A. Szabo. 1981. Diffusion controlled bimolecular reaction rates. The effect of rotational diffusion and orientational constraints. *Biophys. J.* 36:697–714.

Siraganian, R. P., W. A. Hook, and B. B. Levine. 1975. Specific in vitro histamine release from basophils by bivalent haptens: evidence for activation by simple bridging of membrane bound antibody. *Immunochemistry.* 12:149–154.

Wilder, R. L., G. Green, and V. N. Schumaker. 1975. Bivalent hapten-antibody interactions I. A comparison of water soluble and water insoluble bivalent haptens. *Immunochemistry.* 12:39–47.

Zidovetzki, R., Y. Blatt, C. B. J. Glaudemans, B. N. Manjula, and I. Pecht. 1980. A common mechanism of hapten binding to immunoglobulins and their heterologous chain recombinants. *Biochemistry.* 19:2790–2795.